# Hierarchical Causal Structure Learning

Sjoerd Hermes<sup>1,2</sup>, Joost van Heerwaarden<sup>1,2</sup>, Fred van Eeuwijk<sup>1</sup>, Pariya Behrouzi<sup>1</sup>

<sup>1</sup> Mathematical and Statistical Methods, Wageningen University
<sup>2</sup> Plant Production Systems, Wageningen University

#### Abstract

Traditional statistical approaches primarily aim to model associations between variables, but many scientific and practical questions require causal methods instead. These approaches rely on assumptions about an underlying structure, often represented by a directed acyclic graph (DAG). When all variables are measured at the same level, causal structures can be learned using existing techniques. However, no suitable methods exist when data are organized hierarchically or across multiple levels. This paper addresses such cases, where both unit-level and group-level variables are present. These multi-level structures frequently arise in fields such as agriculture, where plants (units) grow within different environments (groups). Building on nonlinear structural causal models, or additive noise models, we propose a method that accommodates unobserved confounders as well as group-specific causal functions. The approach is implemented in the R package HSCM, available at https://CRAN.R-project.org/package=HSCM.

Keywords: Causality, causal discovery, hierarchical data.

## 1 Introduction

Understanding complex real-life phenomena, such as the interplay between plant traits, genotypes, and environmental conditions, requires a statistical framework that moves beyond correlations to one that aims to uncover the underlying causal mechanisms. Structural causal models (SCMs) (Peters et al., 2014; 2017) offer such a framework, as they allow for causal reasoning among variables. Whilst SCMs are promising, many real-life phenomena come with an additional level of complexity that hinders the discovery of causal relations, as these systems are inherently hierarchical: students within schools, patients within hospitals, obligors within banks or plants within environments. This nested structure creates dependencies that standard SCMs do not capture. In addition, it is well-known that unobserved confounders can render estimated causal structures useless and bias estimated causal effects. To this end, the assumption of no unobserved confounders is frequently made, an assumption known in the literature as causal sufficiency (Peters et al., 2017). However, more often than not, this is an untenable assumption.

To address this, we expand on the initial work done by Jensen et al. (2020), Witty et al. (2020) and Weinstein and Blei (2024), all of whom have made contributions to the hierarchical structural causal model (HSCM). These models explicitly account for nested sources of variation, that is at both the group (e.g. environment or school) and unit (e.g. plant or student) levels. Whilst being conceptually useful, all work done on such models assumes that the directed acyclic graph (DAG) corresponding to the causal structure of the phenomenon of interest is known, thereby greatly restricting the applicability of the HSCM on real-world multivariate data. In this paper, we make no such assumption, but instead introduce a new way to learn the causal structure corresponding to a HSCM, which is called causal discovery. The proposed method is able to learn nonlinear relationships within and between all levels of the hierarchy (groups and units). In addition, the method allows for unobserved group-level confounders that affect variables at the unit level. Some further extensions are also proposed in this paper such as group-specific functions, multiple grouping factors and unit-level confounders. We demonstrate the effectiveness of our method on simulated data and a real-world example from agricultural science.

This work contributes to the growing body of literature on tools for causal discovery on observational data. Our hierarchical causal discovery framework is general and applicable across a wide range of nested real-life phenomena, offering a new lens through which to model and interpret these complex datasets. The novelties proposed in this paper are critical for, amongst others, modern agricultural research, where trials increasingly consist of different environments or genotypes (van Eeuwijk et al., 2005; Hermes et al., 2024)

The paper starts with a description of the HSCM model, before extending it to obtain the proposed method in Section 2. Causal structure learning is discussed in Section 3. Section 5 consists of a simulation study that evaluates the performance of the proposed method in terms of causal structure learning; both the causal DAG

and the corresponding causal functions. An application of the proposed method on two agricultural datasets pertaining to maize and winter wheat is provided in Section 6. Finally, Section 7 concludes the article and discusses some potential future extensions of the proposed method.

## 2 Hierarchical Structural Causal Model

To specify the HSCM, we first introduce some notation. The type of variables under consideration are observed group-level variables Z, unobserved group-level variables U and observed unit-level variables X. Let  $\operatorname{Pa}\left(X^{k}\right)$  denote the set of parents of the k-th unit-level variable,  $k=1,\ldots,p$ , and  $\operatorname{Pa}\left(Z^{k}\right)$  denote the set of parents of the k-th group-level variable,  $k=1,\ldots,q$ . We use  $\operatorname{Pa}_{Z}\left(X^{k}\right)$  to denote the parents in Z of  $X^{k}$ . Similarly  $\operatorname{Ch}\left(X^{k}\right)$  and  $\operatorname{Ch}\left(Z^{k}\right)$  denote the children of  $X^{k}$  and  $Z^{k}$ . Whilst the unobserved group-level confounders are assumed to have no parents, their children are given by  $\operatorname{Ch}\left(U^{k}\right)$ ,  $k=1,\ldots,r$ . Even though we use the superscript k for both the unit- and group-level variables,  $X^{k}$  and  $Z^{k}$  represent different variables. To distinguish between the different levels of the hierarchical model, we use subscripts  $i=1,\ldots,n_{j}$  and  $j=1,\ldots,m$  for the units within groups and the groups themselves respectively. For notational simplicity, we assume that  $n_{j}=n'_{j}$  for all  $j\neq j'$ , such that  $i=1,\ldots,n$ . Therefore, we have that  $Z\in\mathbb{R}^{m\times q},U\in\mathbb{R}^{m\times r}$  and  $X\in\mathbb{R}^{nm\times q}$ . Without any additional assumptions or restrictions, the HSCM has the following general form

$$Z^{k} = f\left(\mathbf{Pa}\left(Z^{k}\right), \varepsilon^{k}\right), k = 1, \dots, q,$$

$$X^{k} = f\left(\mathbf{Pa}\left(X^{k}\right), \varepsilon^{k}\right), k = 1, \dots, p,$$
(1)

where  $\mathbf{Pa}\left(Z^k\right) \subset \mathbf{Z}_{\backslash Z^k}$  ( $\backslash Z^k$  implies excluding  $Z^k$ ) and  $\mathbf{Pa}\left(X^k\right) \subset \left(\mathbf{Z} \cup \mathbf{U} \cup \mathbf{X}_{\backslash X^k}\right)$ , and where and  $\varepsilon^k$  represents a noise variable. Any HSCM corresponds to a DAG encompassing the complete causal structure of both the relationships within and between levels. An example of such a DAG is given in Figure 1.

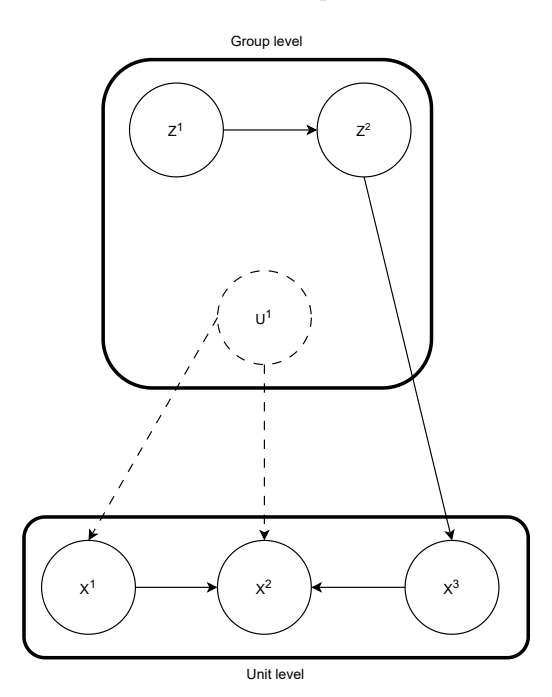


Figure 1: Example of a DAG corresponding to a HSCM with two observed group-level variables, one unobserved group-level confounder and three unit-level variables.

The general form of the HSCM presented in Equation (1) renders a model that is not identifiable (Peters et al., 2014). Therefore, to learn the causal structure, the SCM literature typically makes assumptions on the causal functions being linear or (additive) nonlinear (Bühlmann et al., 2014), and on the noise being for non Gaussian (Shimizu et al., 2006; Leyder et al., 2025) or Gaussian (Park, 2023). Here, we follow Bühlmann et al. (2014) and assume that the causal functions are nonlinear and additive in the variables and error terms.

We first introduce the HSCM found in Witty et al. (2020) and Weinstein and Blei (2024), except that we impose additivity, nonlinearity and Gaussian noise to ensure identifiability (Bühlmann et al., 2014; Peters et al., 2014), before extending it with group-specific functions, additional grouping factors and unit-level confounders. The

HSCM is written as

$$Z^{k} = \sum_{Z^{l} \in \mathbf{Pa}(Z^{k})} f^{l}(Z^{l}) + \varepsilon^{k}$$

$$X_{j}^{k} = \sum_{Z_{j}^{l} \in \mathbf{Pa}(X_{j}^{k})} g^{l}(Z_{j}^{l}) + \sum_{U_{j}^{r} \in \mathbf{Pa}(X_{j}^{k})} h^{l}(U_{j}^{r}) + \sum_{X_{j}^{d} \in \mathbf{Pa}(X_{j}^{k})} s^{d}(X_{j}^{d}) + \xi_{j} + \varepsilon_{j}^{k} \quad j = 1, \dots, m,$$

$$(2)$$

where  $\xi_j$  is a group-specific intercept and  $\varepsilon_j^k \sim N[0, (\sigma_j^k)^2]$ . The  $g(\cdot)$  and  $h(\cdot)$  need not be nonlinear. In fact, assuming linearity tends to lead to better results in practice and does not hinder identifiability. This is because the causal direction is fixed (from group-level variable to unit-level variable), provided a relationship between the two exists. Conversely, the  $f(\cdot)$  and  $s(\cdot)$  are restricted to be nonlinear for identifiability reasons. In contrast to the HSCM proposed by Weinstein and Blei (2024), we do not have a separate noise variable for the between group variation that occurs for the unit-level variables which cannot be explained away by the group-level variables. This is because we use the group-specific intercept (and the group-specific nonlinear unit parents effect in the extended version) to account for this variation. As such, we obtain an equivalence with multilevel or linear mixed models, where the higher level residuals are absorbed into different intercepts. Even though  $\mathbf{Ch}(U_j^r) \geq 1$ , for all j ( $U^r$  is a confounder), this is no problem in causal structure estimation, as for each j, the causal structure of X can be estimated separately (Jensen et al., 2020). Moreover, the structure provided in Equation (2) is robust to omitted variable bias that might be incurred from the unobserved group-level variables  $U^r$ , if we make the following assumption:

**Assumption 1.** Assume that the  $U^r$  affect the  $X^k$  in an additive fashion and that  $Z^l \perp \!\!\! \perp U^r$  for all l, r.

This assumption is required as otherwise, the group-specific intercepts  $\xi_j$  absorb some of the shared variation of both the  $U^r$  and  $Z^l$ , making it impossible to isolate the effect of  $Z^l$  from  $U^r$ , resulting ultimately in an inability to detect the causal parents of the  $X^k$  in Z.

### 2.1 Extending the HSCM

Whilst the HSCM framework provided in Equation (2) already offers a flexible way in which to deal with hierarchical data, some extensions can further increase its applicability. Here, we discuss a few of these.

The first extension is one where group-specific functions are added for the unit-unit relationships. Due to latent causes, the effect of one unit-level variable on another might vary across groups. If an additive group-level intercept is unable to capture these differences, the HSCM can be extended using group-specific functions. Similar to the model presented in Equation (2), the following model is obtained:

$$Z^{k} = \sum_{Z^{l} \in \mathbf{Pa}(Z^{k})} f^{l}\left(Z^{l}\right) + \varepsilon^{k}$$

$$X_{j}^{k} = \sum_{Z^{l} \in \mathbf{Pa}\left(X_{j}^{k}\right)} g^{l}\left(Z_{j}^{l}\right) + \sum_{U_{j}^{r} \in \mathbf{Pa}\left(X_{j}^{k}\right)} h^{r}\left(U_{j}^{r}\right) + \sum_{X_{j}^{d} \in \mathbf{Pa}\left(X_{j}^{k}\right)} s_{1}^{d}\left(X_{j}^{d}\right) + \sum_{X_{j}^{d} \in \mathbf{Pa}\left(X_{j}^{k}\right)} s_{2j}^{d}\left(X_{j}^{d}\right) + \xi_{j} + \varepsilon_{j}^{k} \quad j = 1, \dots, m,$$

$$(3)$$

where  $s_1(\cdot)$  is the global function common to all groups and  $s_{2j}(\cdot)$  is a group-specific function from group j. Rather than omitting the global function, it is included in the extended model provided by Equation (3), as the global function enables prediction for unseen groups.

It is possible that for some groups,  $X_j^k \in \mathbf{Pa}\left(X_j^l\right)$ , but  $X_{j'}^k \notin \mathbf{Pa}\left(X_{j'}^l\right)$ . As such, the effect of  $X_{j'}^k$  on  $X_{j'}^l$  is 0, implying that there is neither a global nor a group-specific causal function for this particular group. Under the following assumption, it is possible to extend the HSCM with this type of relations:

**Assumption 2.** Assume that

$$\left[X_{j}^{k} \in \boldsymbol{Pa}\left(X_{j}^{l}\right) \wedge X_{j'}^{k} \notin \boldsymbol{Pa}\left(X_{j'}^{l}\right) \wedge X_{j'}^{l} \notin \boldsymbol{Pa}\left(X_{j'}^{k}\right)\right]$$

$$\vee \left[X_{j}^{l} \in \boldsymbol{Pa}\left(X_{j}^{k}\right) \wedge X_{j'}^{l} \notin \boldsymbol{Pa}\left(X_{j'}^{k}\right) \wedge X_{j'}^{k} \notin \boldsymbol{Pa}\left(X_{j'}^{l}\right)\right] \quad \forall j \neq j'.$$

Assumption This assumption limits the directionality of the edges in a DAG for different groups. If an edge between two vertices in the DAG exists for some group, its direction is shared by all groups for which that edge exists. This extension of 0-edges for some groups is primarily useful for outlier groups. Suppose that in most cases, applying additional fertiliser to a plant affects its yield, resulting in an edge in the DAG between the vertices corresponding to the fertiliser and yield variables. If there exists some environment which already has a high nitrogen concentration in the soil, additional fertiliser might not affect yield, thus resulting in a lack of

an edge between the vertices corresponding to the fertiliser and yield variables for the group corresponding to the high-nitrogen environment.

Related to this is the possibility to allow for unobserved unit-level confounders. Whilst the HSCM presented by Equation (2) only allows for unobserved group-level confounders that affect unit-level variables, under some mild assumptions, it is possible to allow for unobserved unit-level confounders (that affect unit-level variables). The following assumption is required:

**Assumption 3.**  $\exists j \text{ such that } C \notin \mathbf{Pa}\left(X_{j}^{k}\right) \cap \mathbf{Pa}\left(X_{j}^{l}\right) \text{ whilst } C \in \mathbf{Pa}\left(X_{j'}^{k}\right) \cap \mathbf{Pa}\left(X_{j'}^{l}\right) \text{ for some } j' \text{ for some } unobserved unit-level confounder } C.$ 

Assumption 3 implies that for any unit-level confounded variable there exists some group that is not affected by an unobserved unit-level confounder, whilst the other groups are affected by that confounder. We assume that this assumption holds for all unobserved unit-level confounders, but for each confounder different groups might be unaffected. We can then use the data from that group to orient the edges to and from  $X_{j'}^k$ , for all j', assuming that

**Assumption 4.** If 
$$\exists j$$
 such that  $C \notin \mathbf{Pa}\left(X_{j}^{k}\right) \cap \mathbf{Pa}\left(X_{j}^{l}\right)$  whilst  $C \in \mathbf{Pa}\left(X_{j'}^{k}\right) \cap \mathbf{Pa}\left(X_{j'}^{l}\right)$  and  $X_{j}^{k} \in \mathbf{Pa}\left(X_{j}^{l}\right)$ , then  $X_{j'}^{k} \in \mathbf{Pa}\left(X_{j'}^{l}\right)$  for all  $j' \neq j$ . The same holds if  $X_{j}^{k} \notin \mathbf{Pa}\left(X_{j}^{l}\right)$  and  $X_{j}^{l} \notin \mathbf{Pa}\left(X_{j}^{k}\right)$ , then  $X_{j'}^{k} \notin \mathbf{Pa}\left(X_{j'}^{l}\right)$  and  $X_{j'}^{l} \notin \mathbf{Pa}\left(X_{j'}^{k}\right)$  or  $X_{j}^{l} \in \mathbf{Pa}\left(X_{j}^{k}\right)$ , then  $X_{j'}^{l} \in \mathbf{Pa}\left(X_{j'}^{k}\right)$ .

Assumption 4 states that the relationship between any two unit-level confounded variables that share the same unit-level confounder is the same for all groups. Consequently, it becomes possible to estimate such a relation for a non-confounded group and impose the same structure on the confounded groups.

The HSCM can be generalized to consist of with multiple grouping factors. Suppose that in addition to Z and X, we also have access to W. If there is no relationship between any of the W and Z variables, but there is between the W and X variables, inclusion of another grouping factor is straightforward. We mention this situation because of its prevalence in real-world data, such as plants (unit-level) that grow in some environment (group-level) and have some genotype (group-level), or patients (unit-level) that are in some hospital (group-level) and have some disease (group-level), or students (unit-level) that take exams in some courses (group-level) in some schools (group-level).

# 3 Causal structure learning

This section describes how the causal structure of a HSCM can be learned. Rather than viewing the hierarchical system presented in Equation (2) as a single entity, we can view it as a system of layered but separate entities: the group level and the unit level. Instead of reinventing the wheel, there already exists reliable methods for causal discovery for such single-entity structures (Bühlmann et al., 2014; Peters et al., 2014). In this paper, we make use of the CAM method proposed by Bühlmann et al. (2014) to determine the causal structures for both the group- and unit levels. CAM estimates the DAG corresponding to multivariate data in three steps:

- 1. Preliminary neighbourhood selection to estimate a superset of the of possible parents of each node by computing additive regressions of one variable against all others. This reduces the search space
- 2. Order search using maximum likelihood estimation based on an additive structural equation model with Gaussian errors. Edges are iteratively added that give the largest increase in the likelihood, while making sure the graph stays acyclic.
- 3. Prune the DAG estimated in step 2 using significance tests to remove false positive edges.

CAM enables us to estimate the DAG corresponding to the group-level variables:  $D_Z$ . However, it also enables the estimation of the within-group causal structure:  $D_X$ . This is because of the concept known as object conditioning (Jensen et al., 2020): whenever we condition on the group entity (only evaluate a single group), all units in that group are affected by the same value of the group-level confounder. Therefore, the group-level confounder simply becomes an additive constant within group. As such, for the model presented in Equation (2), where the causal structure is the same for all groups,  $D_X$  can be estimated using the data pertaining to a single group. What is left is to connect the group-level variables to the unit-level variables. This is done using additive regression, where the dependent variables are the unit-level variables and the independent variables are the parents in  $D_X$  and all group-level variables. Group-level intercepts are included to mitigate the omitted variable bias caused by the unobserved group-level confounders. We then assign those group-level variables to be parents of the dependent unit-level variable when the p-value corresponding to the estimated smooth function (denoted as pv(f) for smooth function f) is below some threshold  $\alpha$ , which is typically set to 0.001.

Finally, the causal functions can be estimated using additive regressions after estimating the complete DAG. We cannot re-use the estimated group-unit and unit-unit functions, as these are biased due to the omitted variable bias that the group-level variables (observed and unobserved) cause on the unit-level variables. Only after estimating the causal structure can we de-bias the causal functions.

We denote the use of the CAM operation on group-level data Z to obtain a group-level DAG  $D_Z$  as CAM (Z), and use similar notation for the unit-level. Algorithm 1 succinctly describes the estimation procedure for the model presented in Equation 2.

#### Algorithm 1 HCSM estimation

```
Input: Data Z, X, test threshold \alpha
Output: DAG \hat{D}_{ZX}.
  1: Set D_Z = \operatorname{CAM}(\mathbf{Z}).
  2: Set \tilde{j} = \{j : n_j > n_{j'} \text{ for all } j'\}
 3: Set D_X = \operatorname{CAM}\left(\boldsymbol{X}_{\tilde{i}}\right).
 4: for k \in 1: p do
5: Compute X^k = \sum_{l=1}^q g^l\left(Z^l\right) + \sum_{X^d \in \mathbf{Pa}(X^k)} s^d\left(X^d\right) + \xi
  6:
               if \operatorname{pv}(g^l) \leq \alpha then
Set Z^l \in \operatorname{Pa}(X^k)
  7:
  8:
                end if
  9:
           end for
10:
11: end for
12: Set \hat{D}_{ZX} = \{\hat{D}_Z, \hat{D}_X, \hat{\mathbf{Pa}}_Z(X^k)\}
```

If we do not make the assumption of no unobserved unit-level confounders, as discussed in Section 2.1, we require a method that can detect the presence of unobserved confounders. One such method is CAM-UV (Maeda & Shimizu, 2021). This method can detect the presence of confounders. If such a confounder is discovered, CAM-UV provides a bidirected edge between the variables affected by the confounder. Nevertheless, CAM-UV manages to recover the part of the causal structure that is not influenced by the confounder. The first line of Algorithm 1 does not change, as the unit-level confounders do not affect the group-level DAG. The third line does change, however. Instead of running CAM on the group with the highest number of observations, we run CAM-UV on each group to estimate the unit-level DAG. Then, judging from the bidirected edges, we can identify where the confounders are and what groups are affected by them. By orienting the edges of the groups affected by the confounders using the estimates edges from the non-confounded groups, we obtain the complete unit-level DAG. In line 5, we keep the assumption that the unit-unit relations only consist of global functions, and use the non-confounded group data to estimate these. The data corresponding to the other groups can still be used to estimate the group-unit relationships.

Causal structure learning for the other extensions proposed in Section 2.1, are trivial compared to the aforementioned scenarios. For the group-specific functions, only line 5 in Algorithm 1 changes, as group-specific unit-unit functions should be added. When a second grouping factor  $\boldsymbol{W}$  exists, we estimate its DAG  $D_W$  before estimating  $D_X$  and we include all variables in  $\boldsymbol{W}$  as possible group-level parents of the  $\boldsymbol{X}$  in step 5. Similarly, to allow for mixed type variables, the CAM method can be replaced by MERIT (Yao et al., 2025).

As an aside, researchers might not always want to estimate the DAG  $D_Z$ , but only care about the DAG  $D_X$  and the relations  $Z \to X$ . Either because these group-level variables cannot be intervened upon, or because there are not enough groups in the data to reliably estimate  $D_Z$ . These type of structures can be estimated by omitting line 1 from Algorithm 1.

## 4 Interventions

Even though this article focuses on causal structure learning, the ability to compute the effect of an intervention is one of the distinguishing factors of a causal model (Pearl, 2009). It is for this reason that interventions have received a substantial amount of attention in the scientific literature on causality (Peters & Bühlmann, 2015; Witty et al. (2020; Weinstein & Blei (2024). This article focuses on hard interventions, that is, an intervention in which a fixed value is assigned to the intervened variable (Peters et al., 2017). Whilst computing interventions for a linear structural causal model has a closed form solution (Peters et al., 2017), this is not the case for its nonlinear counterpart. In this paper, we use a simulation-based approach to compute queries of the form

 $\mathbb{P}[X|do(y)]$ , that is, the interventional distribution of some variable X whenever we assign the value y to variable Y. Both outcome and intervened variable can be at the unit- or group level, as long as the intervened variable is not at the unit-level whilst the outcome variable is at the group-level. The method used to compute hard interventions is described succinctly in Algorithm 2, where details are provided in verbose below.

#### Algorithm 2 HCSM computing hard interventions

**Input:** Data Z, X, DAG  $\hat{D}_{ZX}$ , causal functions  $\hat{f}$ , intervened variable Y, intervened value y, group-level simulation samples M, unit-level simulation samples N

```
Output: Intervened data Z, X.
 1: Set Y = y
    for k \in 1 : q do
         if \hat{\mathbf{Pa}}(Z^k) = \emptyset and Z^k \neq Y then
 3:
            for i \in 1 : m \operatorname{do}
 4:
 5:
                Draw, by resampling, M samples from Z_i^k
            end for
 6:
         end if
 7:
 8: end for
 9: for k \in \hat{\pi}_Z do
         if Z^k \neq Y then
10:
            for i \in 1 : m do
11:
                for j \in 1 : M do
12:
                   Draw \varepsilon_{ij}^k \sim N(0, \hat{\sigma}_k^2)
13:
                   Set Z_{ij}^{k} = \sum_{Z^{l} \in \hat{\mathbf{Pa}}(Z^{k})} \hat{f}^{l} \left( Z_{ij}^{l} \right) + \varepsilon_{ij}^{k}
14:
15:
            end for
16:
17:
         end if
18: end for
19: for k \in 1 : q do
20:
         for i \in 1 : m \operatorname{do}
            for j \in 1 : M do
21:
                Replicate each Z_{ij}^k N times.
22:
            end for
23:
24:
         end for
25: end for
     for k \in 1 : p do
26:
         if \hat{\mathbf{Pa}}(X^k) = \emptyset and X^k \neq Y then
27:
            for i \in 1 : m \operatorname{do}
28:
29:
                for j \in 1 : M do
                   Draw, by resampling, N samples from X_{ij}^k
30:
                end for
31:
32:
            end for
33:
         end if
34: end for
35: for k \in \hat{\pi}_X do
         if X^k \neq Y then
36:
            for i \in 1 : m do
37:
                for j \in 1 : M do
38:
                   for r \in 1: N do
39:
                       Draw \varepsilon_{ijr}^k \sim N(0, \hat{\sigma}_k^2)
40:
                       Set X_{ijr}^{k} = \sum_{Z^{l} \in \mathbf{Pa}(X^{k})} \hat{g}^{l} \left( Z_{ijr}^{l} \right) + \sum_{X^{d} \in \mathbf{Pa}(X^{k})} \hat{s}^{d} \left( X_{ijr}^{d} \right) + \hat{\xi}_{i} + \varepsilon_{ijr}^{k}
41:
                   end for
42:
                end for
43:
            end for
44:
45:
         end if
46: end for
```

To sample from an interventional distribution after a hard intervention, the causal DAG  $D_{ZX}$  needs to be estimated beforehand, together with the causal functions f. As interventional distributions are computed using simulation, we need to set the number of group- and unit-level simulation samples beforehand, which are denoted by M and N respectively. The proposed method relies on resampling observations for parentless

variables, see lines 5 and 30 of Algorithm 2. Whilst resampling observations across group at the unit-level is not allowed, as these observations are not exchangeable across groups, resampling group-level observations across groups is allowed, as these are exchangeable.

The algorithm commences by fixing the intervened variable Y at the chosen hard intervention value y. Y can be either a group- or unit-level variable. Subsequently, for each group m, the group-level variables  $Z^k$  which have no parents, M samples (subgroups) are drawn with replacement from the observed  $Z^k$ . This results in mM observations at the group level rather than M observations, which would be typical in a resampling or bootstrap context. The reasoning behind this is that the original m groups should be maintained as this is crucial to the unit-level variables, which are nested in the group level, and sampling of these depends on group-specific intercepts, which are only estimated for the original m groups.

The next step consists of sampling the other group-level variables according to their position in the causal order. Corresponding to the model defined in Equation 2, we first draw the residuals from a normal distribution with mean 0 and plug in the estimated variance. We then assign a value of the group-level variable using its estimated parents together with the residual.

The unit-level variables are sampled in a similar way, except that the parentless unit-level variables are resampled using only the observations found in their own group. Moreover, we draw N samples at the unit-level for each subgroup (M) per group (m), resulting in a total number of mMN observations instead of the original mn observations.

# 5 Simulation study

The effectiveness of the proposed method is demonstrated by means of a simulation study. Data is simulated according to the model given by Equation 3. First, the causal graph is generated to determine the causal order. The causal graph consists of  $q \in \{4, 10\}$  observed group-level variables,  $r \in \{1, 2\}$  unobserved group-level variables and  $p \in \{4, 10\}$  observed unit-level variables. To generate both the observed group-level and unit-level DAGs, respectively  $D_Z$  and  $D_X$ , either 2 or 5 edges are randomly sampled, depending on whether p = q = 4 or p = q = 10 respectively. Subsequently, the same number of edges are sampled between any of the group-level and unit-level variables. Finally, either 2 or 4 edges are sampled from the unobserved group-level variables to the unit-level variables, depending on whether 1 or 2 unobserved group-level variables are generated respectively.

With the full DAG created the data can be simulated. The data consist of  $m \in \{25, 50, 100, 250\}$  groups and  $n \in \{25, 50, 100, 250\}$  units within groups. All data for the group-level variables are simulated first, starting with the source variables (variables without parents), which only consist of a (standard normal) noise variable. The other group level variables are simulated according to the causal order corresponding with  $D_Z$ . The nonlinear functions used are the sin, squared, cubic, exponential relu and softplus functions, where is function is randomly assigned a positive or negative sign and a coefficient in [0.5, 2]. Similarly, the data for the unit-level variables are generated starting with the source variables. Subsequently, the other unit-level variables are generated following the causal order in  $D_X$ , combined with the group-level parents of the unit-level variables. The same nonlinear functions with a random sign and coefficient that were used for the group-level variables are used to generate the unit-level variables.

The HSCM is fitted on the generated data. Its performance is evaluated by means of the Structural Hamming Distance (SHD) and the root mean squared error (RMSE). The SHD is used as an error metric for the causal structure, that is, how does the estimated DAG  $\hat{D}_{ZX}$  compare to the true dag  $D_{ZX}^0$ , whereas the RMSE is used as an error metric for the estimated causal functions. Whilst the RMSE is well-known to the general audience, the SHD is not. The SHD counts the number of operations required to go from the estimated DAG  $\hat{D}_{ZX}$  to the true dag  $D_{ZX}^0$ . The RMSE for the causal functions is estimated by evaluating the true and estimated functions on the same set of values and computing the RMSE on the respective outcomes. For each simulation setting consisting of different n, m, p and q, the model is fitted on 50 generated datasets. Results for this simulation study are provided in Table 1. Additional simulation results, for data generated with group-specific functions and with an additional grouping factor W, are provided in the Appendix.

Table 1: Results for the proposed method. The SHD and RMSE are averaged across 50 randomly generated datasets.

	l giib	DATGE
n, m, p, q	SHD	RMSE
25, 25, 4, 4	2.88 (0.19)	0.10(0.01)
50, 25, 4, 4	2.42 (0.18)	0.11(0.01)
100, 25, 4, 4	2.26 (0.17)	0.11 (0.01)
250, 25, 4, 4	1.88 (0.16)	0.08(0.01)
25, 50, 4, 4	2.62 (0.23)	0.11(0.01)
50, 50, 4, 4	2.18 (0.21)	0.13(0.02)
100, 50, 4, 4	1.56 (0.15)	0.08(0.01)
250, 50, 4, 4	1.20 (0.20)	0.09(0.01)
25, 100, 4, 4	2.20 (0.22)	0.10(0.01)
50, 100, 4, 4	1.64 (0.19)	$0.11 \ (0.01)$
100, 100, 4, 4	1.26 (0.16)	0.09(0.01)
250, 100, 4, 4	0.90 (0.18)	0.08 (0.01)
25, 250, 4, 4	1.94 (0.20)	$0.11 \ (0.01)$
50, 250, 4, 4	1.46 (0.17)	$0.11 \ (0.01)$
100, 250, 4, 4	0.74 (0.11)	0.08(0.01)
250, 250, 4, 4	0.52 (0.13)	0.08(0.01)
25, 25, 10, 10	8.82 (0.33)	$0.11 \ (0.01)$
50, 25, 10, 10	7.42 (0.35)	$0.10 \ (0.01)$
100, 25, 10, 10	6.42 (0.28)	$0.10 \ (0.01)$
250, 25, 10, 10	5.68 (0.30)	$0.10 \ (0.01)$
25, 50, 10, 10	7.60 (0.29)	$0.10 \ (0.01)$
50, 50, 10, 10	6.00 (0.36)	$0.10 \ (0.01)$
100, 50, 10, 10	5.16 (0.38)	$0.10 \ (0.01)$
250, 50, 10, 10	3.82 (0.29)	0.09(0.01)
25, 100, 10, 10	7.26 (0.40)	$0.10 \ (0.01)$
50, 100, 10, 10	4.96 (0.32)	$0.10 \ (0.01)$
100, 100, 10, 10	4.10 (0.31)	$0.10 \ (0.01)$
250, 100, 10, 10	3.50 (0.35)	0.09(0.01)
25, 250, 10, 10	5.70 (0.35)	0.09(0.01)
50, 250, 10, 10	4.36 (0.34)	$0.10 \ (0.01)$
100, 250, 10, 10	2.82 (0.27)	0.09(0.01)
250, 250, 10, 10	2.30 (0.29)	0.11 (0.01)

From the results provided in Table 1, it appears that the proposed structure learning method is capable of learning both the causal structure and the functions corresponding to data as generated by Equation 3, provided that enough data is supplied to the model. The estimation error for the causal functions appears to be more-or-less constant, around 0.10. This is likely because the main problem is within the learning of the structure itself, and it is relatively simple to learn the causal functions, as this amounts to a regression problem. As such, the RMSE is more or less constant throughout all simulation settings.

The computation time is evaluated on 50 datasets where p = q = 10 and r = 2, with different values for n and m. The results are shown in Figure 2.

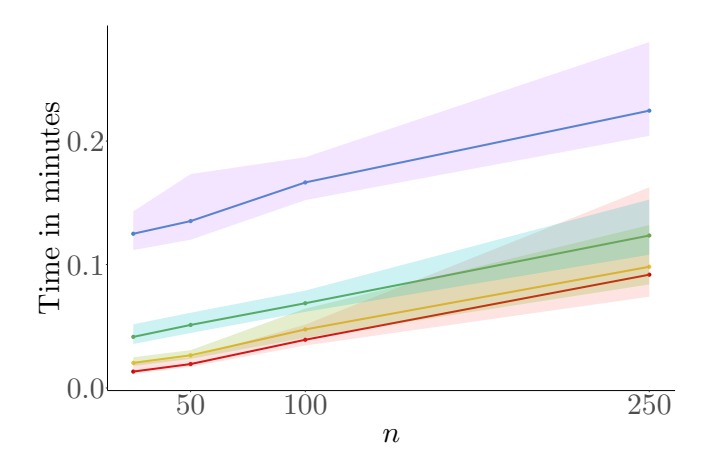


Figure 2: Computation time for the proposed method in minutes. The colours represent the values of m: 25 \_\_\_\_\_, 50 \_\_\_\_, 100 \_\_\_\_ and 250 \_\_\_\_. The solid lines reflect the average times across 50 fitted models, whereas the shading around the lines reflect the minimum and maximum computation times across the fitted models.

## 6 Applications on maize and winter wheat data

We illustrate the proposed method using two different agricultural datasets: one pertaining to maize in Ethiopia (Silva et al., 2023) and another one pertaining to winter wheat in Switzerland (Roth et al., 2025). Both datasets consist of measurements across plots containing plants, the unit-level, which are nested either within different geographical locations (districts) for the maize data, or within different years for the winter wheat data. Each of these groupings can cause heterogeneity in the growing environment for the plants, as they can correspond to different (unmeasured) weather and soil properties.

Whilst numerous variables are included in both datasets, the central variable in each of them is the yield variable, measured at unit-level. Yield is a complex plant trait that is frequently thought to be some function of a plant's genotype (G), the growing environment (E) and human management (M) (Hermes et al., 2023; 2024). The reason as to why yield is so central in agricultural research should not come as surprising, as it is the primary driver in global food security (Fischer et al., 2014). In addition to yield, the datasets contain variables describing each of the G, E and M factors, such as the plant height (G), precipitation (E) and the seed rate (M). The maize data contains 13 variables, whilst the winter wheat data contains 11 variables. Moreover, the maize data consists of 37 different districts, with each group containing between 5 and 84 units (average of 28), and the winter wheat data consists of 4 different years, with each group containing between 305 and 634 units (average of 459). Whilst the dimensionality maize data seems to be similar to the dimensionality used in the simulation study described in Section 5, the number of groups for the winter wheat data is very small. In fact, it is prohibitively small, so that the group-level DAG  $D_Z$  cannot be reliably estimated. Instead, for the winter wheat data, we do not estimate  $D_Z$ , but only estimate the relations  $Z \to X$  and  $D_X$  to avoid making any (probably) false claims w.r.t.  $D_Z$ . Conversely, the full causal structure is estimated for the maize data. We believe that these differing aims showcase the versatility of the proposed method, which can still provide useful insights even if the number of groups is small.

The proposed method is fitted on both datasets, resulting in the causal structures presented in Figures 3a and 3b for the maize and winter wheat data respectively.

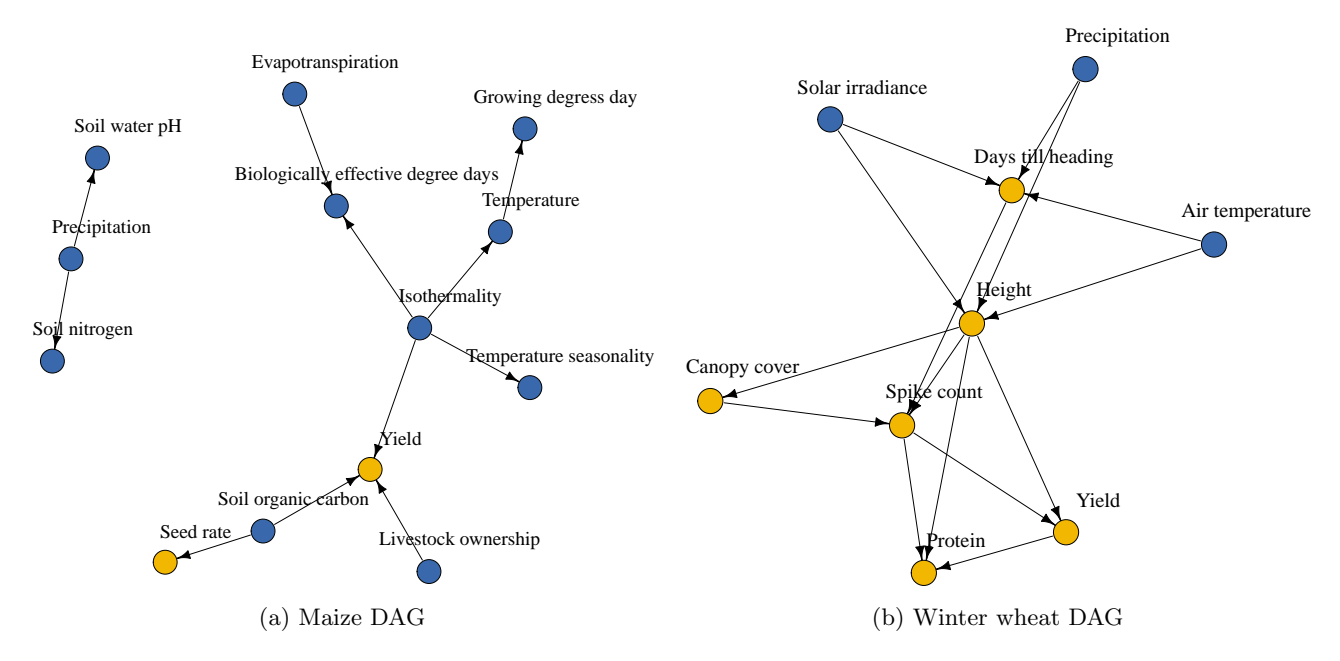


Figure 3: Estimated DAGs for both datasets. Unit-level variables are represented by yellow vertices, whilst group-level variables are represented by blue ones

Both causal structures in Figures 3a and 3b provide us with some interesting results. Focusing on yield, both causal structures identify yield to be a complex trait that is caused by numerous other variables, both at the group-level in the case of the maize data, as well as the unit-level in case of the winter wheat data. The results for maize correspond to typical findings (Hermes et al., 2023; 2024), in which yield is found to be governed by soil properties and weather. Livestock ownership also emerges as a parent of yield, likely reflecting indirect effects such as manure availability or farmer wealth. Perhaps more interesting is how various plant traits influence each other. This is represented by Figure 3b, which illustrates the estimated causal structure for winter wheat. Yield appears to be a variable that is caused by plant traits such as height and the (wheat) spike count. Where this latter effect reversed, e.g. yield causes spike count, the causal structure would become implausible. Yield does not appear to be directly affected by weather-related variables, but only through these intermediary variables. Surprisingly, yield appears to cause protein content, contrasting with the common assumption that nitrogen drives both (Terman, 1979; Fischer et al., 1993), which is not measured here.

In addition to the causal structure, the proposed method can learn the corresponding causal functions. For both datasets, we assumed group-specific functions for the unit-unit relationships. The group-specific relationships that cause yield for winter wheat are shown in Figures 4a and 4b. No relationships are shown for the maize data, as yield is not influence by any other unit-level variables.

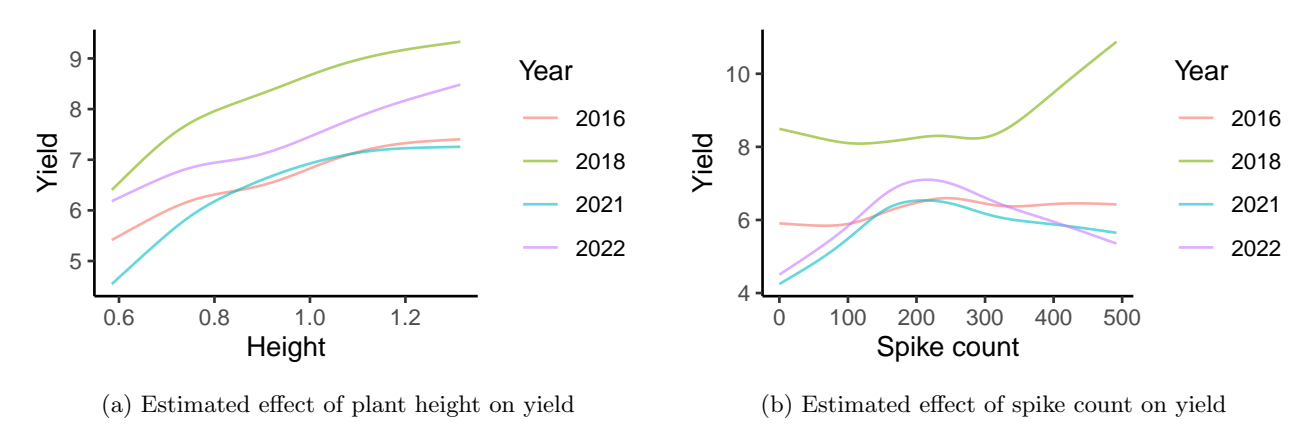


Figure 4: Estimated group specific effects for the winter wheat yield.

The effect of plant height on yield shown in Figure 4a appears relatively simple: the relationships are almost linear and the differences between groups can be captured by a mean-shift. Moreover, these relationships are positive: higher plant heights cause higher yields. Conversely, the relationship between spike count and yield shown in Figure 4b appears to be much more complex: the relationships are highly nonlinear, and groups differ

not just in mean response, but also in the shape of the causal function. In 2018, yields appear to increase as a function of higher spike counts, whilst this is only true for spike counts up until 200 in 2022, after which yields decrease with increasing spike counts.

As mentioned in Section 4, it is possible to compute the interventional distribution for any hard intervention on a HSCM using Algorithm 2. We illustrate such interventions for the winter wheat data, where we intervene on the plant height and the spike count, by setting these to 3 and 1000 respectively. Algorithm 2 is applied on the estimated DAG and the corresponding causal functions for the winter wheat data, where we set M=N=500 for both interventions. The resulting interventional distributions are shown in Figures 5a and 5b.

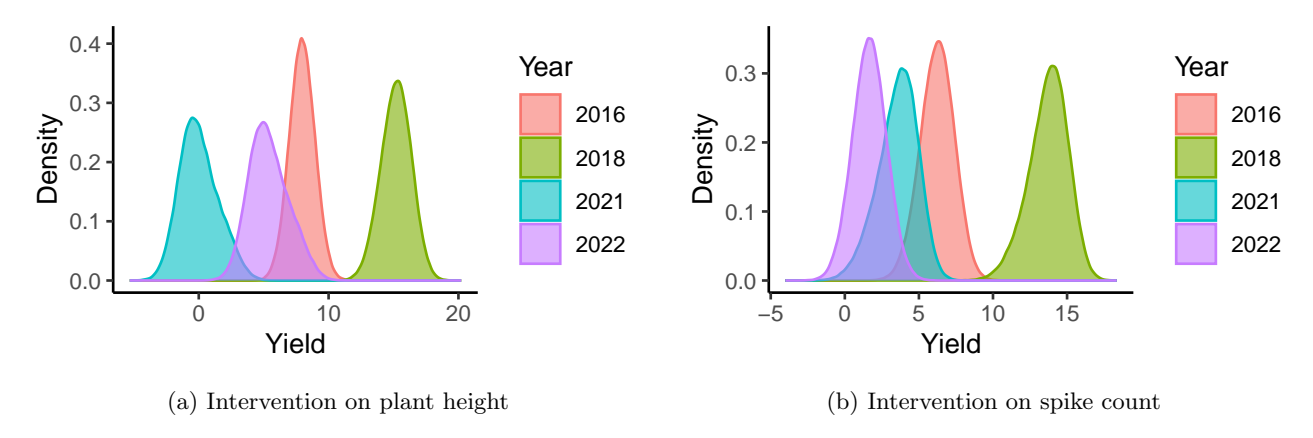


Figure 5: Estimated interventional distributions of winter wheat yield.

### 7 Conclusion

In this work, we have introduced a general framework for hierarchical causal structure learning that extends existing structural causal models to settings where data are nested across multiple levels. By allowing for unobserved confounders, group-specific causal functions, and multiple grouping factors, the proposed approach provides a flexible and realistic way to uncover causal mechanisms in complex hierarchical systems. Through simulation studies, we demonstrated that the method performs well in recovering both causal structures and functional relationships, provided that sufficient data are available. Applications to real-world agricultural datasets further illustrated its capacity to reveal meaningful causal insights in domains where hierarchical variation is the norm.

Beyond methodological innovation, our contribution has practical significance. Hierarchical causal discovery is increasingly relevant in fields such as agriculture, education, epidemiology, and the social sciences, where nested structures are unavoidable. By embedding this approach in the HSCM R package, we have also aimed to make these advances directly accessible to applied researchers. The empirical results on maize and winter wheat data underscore the method's ability to go beyond simple correlation-based analysis and provide interpretable causal explanations that can inform decision-making in breeding, management, and policy.

Looking ahead, there are several promising directions for future research. From a methodological perspective, extending the framework to better handle dynamic hierarchical systems could further expand its applicability. Investigating theoretical properties such as identifiability under weaker assumptions, or improving computational efficiency for high-dimensional settings, also remain important challenges. From an applied perspective, testing the method in fields beyond agriculture—such as healthcare, economics, and environmental science—can help establish its broader utility. Finally, combining hierarchical causal discovery with predictive modeling frameworks may open the door to hybrid approaches that are both explanatory and predictive.

In sum, this work provides both a theoretical advance and a practical tool for causal discovery in hierarchical data. By bridging the gap between causal modeling and real-world nested structures, it contributes to a growing effort to make causal inference more robust, more general, and more useful in the complex systems that shape our scientific and societal challenges.

# Appendix A: Additional simulation results

In addition to the simulations for the baseline model, that is the model presented by Equation 2, causal structure learning for the proposed extensions is shown by means of additional simulations, whose results are presented in Table A1. The data generating mechanism is exactly the same as that for the simulations in Section 5, except

that the additional W has the same number of variables and confounders as Z, and that the group-specific functions are set to equal the global function multiplied by a randomly drawn sign multiplied by a randomly drawn coefficient.

Table A1: Results for the proposed method. The SHD and RMSE are averaged across 50 randomly generated datasets.

	W		Group-specific functions	
obs group, obs unit, vars	SHD	RMSE	SHD	RMSE
25, 25, 4	5.44 (0.27)	0.15 (0.04)	2.94 (0.17)	0.48 (0.04)
50, 25, 4	4.70(0.23)	0.11(0.01)	2.52(0.15)	0.51(0.04)
100, 25, 4	3.34 (0.29)	0.11(0.01)	2.32(0.16)	0.45 (0.03)
250, 25, 4	2.74(0.24)	0.09(0.01)	2.24 (0.20)	0.45 (0.03)
25, 50, 4	4.60 (0.26)	0.09(0.01)	2.44 (0.18)	0.35(0.04)
50, 50, 4	3.84 (0.23)	0.11(0.01)	2.08 (0.17)	0.51 (0.05)
100, 50, 4	2.60 (0.29)	0.11(0.01)	1.76(0.15)	$0.50 \ (0.05)$
250, 50, 4	2.22(0.27)	0.12(0.01)	1.94 (0.20)	0.48(0.04)
25, 100, 4	4.24 (0.27)	0.11(0.01)	2.00(0.14)	0.36 (0.03)
50, 100, 4	3.08 (0.21)	0.11(0.01)	1.66 (0.18)	0.42(0.02)
100, 100, 4	2.44 (0.28)	0.13(0.01)	1.40 (0.16)	0.43 (0.03)
250, 100, 4	1.92 (0.29)	0.11(0.01)	1.12 (0.16)	0.45 (0.03)
25, 250, 4	4.02 (0.21)	0.10(0.01)	1.50(0.12)	0.41 (0.04)
50, 250, 4	2.64 (0.20)	0.11(0.01)	1.15(0.13)	0.42(0.02)
100, 250, 4	1.96 (0.27)	0.13(0.01)	1.06(0.13)	0.38(0.04)
250, 250, 4	1.22 (0.22)	0.13(0.01)	1.00 (0.10)	0.32(0.02)
25, 25, 10	13.46 (0.34)	0.10(0.01)	8.84 (0.23)	0.48 (0.03)
50, 25, 10	10.28 (0.43)	0.11(0.01)	8.48 (0.28)	0.48 (0.03)
100, 25, 10	10.32 (0.46)	0.12(0.01)	7.22(0.28)	0.46 (0.02)
250, 25, 10	8.44 (0.54)	0.09(0.01)	6.28 (0.26)	0.41(0.02)
25, 50, 10	12.26 (0.47)	0.10(0.01)	6.64 (0.34)	0.52 (0.03)
50, 50, 10	9.72(0.45)	0.10(0.01)	6.12(0.26)	0.51 (0.03)
100, 50, 10	9.16 (0.48)	0.11(0.01)	5.28(0.32)	0.48 (0.02)
250, 50, 10	6.82 (0.54)	0.11(0.01)	4.20 (0.24)	0.42(0.02)
25, 100, 10	12.58 (0.50)	0.09(0.01)	5.66(0.24)	0.50 (0.04)
50, 100, 10	8.90 (0.42)	0.13(0.01)	4.98(0.26)	0.47(0.03)
100, 100, 10	6.78 (0.46)	0.11(0.01)	4.16 (0.28)	0.49(0.03)
250, 100, 10	6.72 (0.58)	0.11 (0.01)	3.40 (0.26)	$0.38 \ (0.02)$
25, 250, 10	10.96 (0.41)	0.10(0.01)	4.52 (0.27)	$0.40 \ (0.02)$
50, 250, 10	7.62 (0.43)	0.12(0.01)	4.23 (0.29)	0.39(0.03)
100, 250, 10	6.16 (0.51)	0.12(0.01)	3.50 (0.21)	$0.35 \ (0.03)$
250, 250, 10	4.72 (0.47)	$0.13 \ (0.01)$	3.05 (0.24)	$0.30 \ (0.03)$

In addition to the simulations where all model assumptions are met, we also illustrate causal structure learning in case of model misspecification. Here, instead of normal residuals, all residuals are drawn from U(-1,1). The results are presented in Table A2

Table A2: Results for the proposed method under misspecified settings. The SHD and RMSE are averaged across 50 randomly generated datasets.

n,m,p,q	SHD	RMSE		
25, 25, 4, 4	3.84 (0.22)	0.17(0.03)		
50, 25, 4, 4	3.74 (0.23)	0.15(0.03)		
100, 25, 4, 4	3.72 (0.20)	0.15(0.02)		
250, 25, 4, 4	3.42 (0.21)	0.16(0.03)		
25, 50, 4, 4	2.98 (0.16)	0.11(0.01)		
50, 50, 4, 4	2.84 (0.21)	0.10(0.01)		
100, 50, 4, 4	2.58 (0.19)	0.09(0.01)		
250, 50, 4, 4	2.78(0.24)	0.11(0.02)		
25, 100, 4, 4	2.98 (0.21)	0.12(0.02)		
50, 100, 4, 4	2.70 (0.23)	0.11(0.02)		
100, 100, 4, 4	3.06 (0.26)	0.13(0.03)		
250, 100, 4, 4	2.78 (0.28)	0.12(0.03)		
25, 250, 4, 4	2.58 (0.18)	0.08(0.01)		
50, 250, 4, 4	1.90 (0.20)	0.07(0.01)		
100, 250, 4, 4	1.80 (0.18)	0.08(0.02)		
250, 250, 4, 4	2.10 (0.20)	0.08(0.01)		
25, 25, 10, 10	9.78 (0.28)	0.12(0.01)		
50, 25, 10, 10	8.86 (0.32)	0.10(0.01)		
100, 25, 10, 10	8.88 (0.46)	0.10(0.01)		
250, 25, 10, 10	8.22 (0.38)	0.09(0.01)		
25, 50, 10, 10	9.14 (0.35)	0.11 (0.01)		
50, 50, 10, 10	8.10 (0.36)	0.11 (0.01)		
100, 50, 10, 10	7.16 (0.41)	0.10(0.01)		
250, 50, 10, 10	6.88 (0.36)	0.09(0.01)		
25, 100, 10, 10	8.52 (0.44)	$0.10 \ (0.01)$		
50, 100, 10, 10	6.40 (0.47)	0.10(0.01)		
100, 100, 10, 10	6.52 (0.51)	$0.10 \ (0.01)$		
250, 100, 10, 10	6.34 (0.46)	$0.10 \ (0.01)$		
25, 250, 10, 10	7.56 (0.29)	0.08 (0.01)		
50, 250, 10, 10	6.16 (0.34)	0.08 (0.01)		
100, 250, 10, 10	5.30 (0.43)	$0.08 \; (0.01)$		
250, 250, 10, 10	5.16 (0.47)	$0.08 \; (0.01)$		

# Appendix B: Extensions

It is worth mentioning that the HSCM can be extended to infer causal relations between mixed (continuous and discrete) variables. by following the approach of Yao et al., (2025). We assume that for any discrete variable  $X^k$  with S unique categories, the following equation holds

$$X^{k} = \operatorname*{arg\,max}_{s=1,\dots,S} \left[ \sum_{X^{l} \in \mathbf{Pa}(X^{k})} f^{l,s}\left(X^{l}\right) + \varepsilon^{k,s} \right],$$

where each category consists of different causal functions and additive noise.

### References

Bühlmann, P., J. Peters, and J. Ernest (2014). Cam: Causal additive models, high-dimensional order search and penalized regression. *The Annals of Statistics*, 2526–2556.

Fischer, R., D. Byerlee, and G. Edmeades (2014). Crop yields and global food security. *ACIAR: Canberra*, *ACT*, 8–11.

- Fischer, R., G. Howe, and Z. Ibrahim (1993). Irrigated spring wheat and timing and amount of nitrogen fertilizer. i. grain yield and protein content. *Field Crops Research* 33(1-2), 37–56.
- Hermes, S., J. van Heerwaarden, and P. Behrouzi (2023). Using copula graphical models to detect the impact of drought stress on maize and wheat yield. *in silico Plants* 5(1), diad008.
- Hermes, S., J. van Heerwaarden, and P. Behrouzi (2024). Copula graphical models for heterogeneous mixed data. *Journal of Computational and Graphical Statistics* 33(3), 991–1005.
- Jensen, D., J. Burroni, and M. Rattigan (2020). Object conditioning for causal inference. In *Uncertainty in Artificial Intelligence*, pp. 1072–1082. PMLR.
- Leyder, S., J. Raymaekers, and T. Verdonck (2025). Tslingam: Directlingam under heavy tails. *Journal of Computational and Graphical Statistics* 34(2), 437–447.
- Maeda, T. N. and S. Shimizu (2021). Causal additive models with unobserved variables. In *Uncertainty in Artificial Intelligence*, pp. 97–106. PMLR.
- Park, G. (2023). Computationally efficient learning of gaussian linear structural equation models with equal error variances. *Journal of Computational and Graphical Statistics* 32(3), 1060–1073.
- Pearl, J. (2009). Causality. Cambridge university press.
- Peters, J. and P. Bühlmann (2015). Structural intervention distance for evaluating causal graphs. *Neural computation* 27(3), 771–799.
- Peters, J., D. Janzing, and B. Schölkopf (2017). Elements of causal inference: foundations and learning algorithms. The MIT Press.
- Peters, J., J. M. Mooij, D. Janzing, and B. Schölkopf (2014). Causal discovery with continuous additive noise models. *The Journal of Machine Learning Research* 15(1), 2009–2053.
- Roth, L., M. Boss, N. Kirchgessner, H. Aasen, B. P. Aguirre-Cuellar, P. P. A. Akiina, J. Anderegg, J. G. Castillo, X. Chen, S. Corrado, et al. (2025). The fip 1.0 data set: Highly resolved annotated image time series of 4,000 wheat plots grown in 6 years. *GigaScience* 14, giaf051.
- Shimizu, S., P. O. Hoyer, A. Hyvärinen, A. Kerminen, and M. Jordan (2006). A linear non-gaussian acyclic model for causal discovery. *Journal of Machine Learning Research* 7(10).
- Silva, J. V., J. van Heerwaarden, P. Reidsma, A. G. Laborte, K. Tesfaye, and M. K. van Ittersum (2023). Big data, small explanatory and predictive power: Lessons from random forest modeling of on-farm yield variability and implications for data-driven agronomy. *Field Crops Research* 302, 109063.
- Terman, G. (1979). Yields and protein content of wheat grain as affected by cultivar, n, and environmental growth factors 1. Agronomy Journal 71(3), 437–440.
- van Eeuwijk, F. A., M. Malosetti, X. Yin, P. C. Struik, and P. Stam (2005). Statistical models for genotype by environment data: from conventional anova models to eco-physiological qtl models. *Australian Journal of Agricultural Research* 56(9), 883–894.
- Weinstein, E. N. and D. M. Blei (2024). Hierarchical causal models. arXiv preprint arXiv:2401.05330.
- Witty, S., K. Takatsu, D. Jensen, and V. Mansinghka (2020). Causal inference using gaussian processes with structured latent confounders. In *International Conference on Machine Learning*, pp. 10313–10323. PMLR.
- Yao, R., T. Verdonck, and J. Raymaekers (2025). Causal discovery in mixed additive noise models. In *International Conference on Artificial Intelligence and Statistics*, pp. 3088–3096. PMLR.